

## **General Disclaimer**

### **One or more of the Following Statements may affect this Document**

- This document has been reproduced from the best copy furnished by the organizational source. It is being released in the interest of making available as much information as possible.
- This document may contain data, which exceeds the sheet parameters. It was furnished in this condition by the organizational source and is the best copy available.
- This document may contain tone-on-tone or color graphs, charts and/or pictures, which have been reproduced in black and white.
- This document is paginated as submitted by the original source.
- Portions of this document are not fully legible due to the historical nature of some of the material. However, it is the best reproduction available from the original submission.

DIST. CATEGORY UC-63  
DOE/JPL-956786/84/2  
DRD NO. SE5  
DRL NO. 212

9950-991

DEVELOPMENT OF HIGH-EFFICIENCY  
SOLAR CELLS ON SILICON WEB

A. Rohatgi, D. L. Meier, R. B. Campbell,  
D. N. Schmidt and P. Rai-Choudhury

Second Quarterly Progress Report  
July to September, 1984

This work was performed for the  
Jet Propulsion Laboratory

Contract No. 956786

November 21, 1984


(NASA-CR-174435) DEVELOPMENT OF HIGH  
EFFICIENCY SOLAR CELLS ON SILICON WEB  
Quarterly Progress Report, Jul. - Sep. 1984  
(Westinghouse Research and) 34 p  
HC A03/MF A01

N85-19521

Unclassified  
14310

CSCI 10A G3/44



 Westinghouse R&D Center  
1310 Beulah Road  
Pittsburgh, Pennsylvania 15235

DIST. CATEGORY UC-63  
DOE/JPL-956786/84/2  
DRD NO. SE5  
DRL NO. 212

DEVELOPMENT OF HIGH-EFFICIENCY  
SOLAR CELLS ON SILICON WEB

A. Rohatgi, D. L. Meier, R. B. Campbell,  
D. N. Schmidt and P. Rai-Choudhury

Second Quarterly Progress Report  
July to September, 1984

This work was performed for the  
Jet Propulsion Laboratory

Contract No. 956786

November 21, 1984



Westinghouse R&D Center  
1310 Beulah Road  
Pittsburgh, Pennsylvania 15235

## TABLE OF CONTENTS

LIST OF FIGURES.....	iii
1. SUMMARY.....	1
2. INTRODUCTION.....	3
3. TECHNICAL PROGRESS.....	5
3.1 Effect of Residual Stress on WEB SPV Diffusion Length.....	5
3.2 Dendritic Web Silicon Solar Cell Fabrication.....	7
3.3 Interaction of Twin Planes with Grown-In Impurities.....	7
3.3.1 DLTS Measurements on Schottky Barrier Diodes Fabricated on Beveled Web Surface.....	7
3.3.2 DLTS Measurements on Schottky Barrier Diodes Formed After Step Etching the Ti-Doped Web Crystal.....	15
3.4 Electron-Beam-Induced Current (EBIC) Measurements to Investigate the Recombination Activity at the Twin Planes in Web Silicon.....	15
3.4.1 EBIC Measurements on Baseline Web Crystals.....	17
3.4.2 EBIC Measurements on Titanium-Doped Web Crystal....	21
4. PROGRAM STATUS.....	25
4.1 Present Status.....	25
4.2 Future Activity.....	25
5. REFERENCES.....	27
6. ACKNOWLEDGMENTS.....	28



# LIST OF FIGURES

	<u>Page</u>
Figure 1. DLTS detection and identification of impurities piled up at the twin plane.....	9
Figure 2. Optical photograph (50X) of beveled sample for Ti-doped web crystal J167-1.1 (run TP-3, sample T-1)...	11
Figure 3. Mask for twin plane activity.....	12
Figure 4. DLTS scan for Ti-doped web crystal J167-1.1, as grown. Test device is a 30-mil Schottky dot.....	13
Figure 5. DLTS study of the interaction between grown-in titanium impurity and the twin planes in dendritic web silicon.....	16
Figure 6. Electron-beam-induced current (EBIC) picture of the beveled baseline web crystal R461-4. Twin planes can be seen on the polished beveled surface.....	18
Figure 7. EBIC scan through the twin planes on the chemically etched region of the beveled web surface of baseline crystal R461-4 ( $I_b \sim 270$ pA).....	19
Figure 8. EBIC scan through the twin planes located on the polished beveled web surface of crystal R461-4. Scan is taken 400 $\mu$ m away from the etched region ( $I_b = 270$ pA).....	20
Figure 9. EBIC scan through the twin planes located on the polished web surface of crystal R461-4. This scan was taken 700 $\mu$ m away from the bottom edge ( $I_b = 270$ pA).....	21
Figure 10. EBIC scan through the twin planes located on the chemically etched region of the beveled web surface of Ti-doped web crystal J167-1.3-TP3#8.....	23
Figure 11. EBIC scan through the twin planes located on the polished region of the beveled web surface of Ti-doped web crystal J167-1.3-TP3#8.....	24

## 1. SUMMARY

The major objective of this contract is to improve web base material with a goal toward obtaining solar cell efficiencies in excess of 18% (AM1). The program consists of the investigation of carrier loss mechanisms in web silicon, development of techniques to reduce carrier recombination in web, and web cell fabrication using effective surface passivation.

During this period the effect of stress on web cell performance has been investigated. Preliminary data indicate that stress has no appreciable influence on the minority-carrier diffusion length in the as-grown web crystals. The diffusion length was found to be about  $30 \pm 10 \mu\text{m}$  in the web crystals with a stress level of  $40 \text{ MDyne/cm}^2$ , as well as in the web crystals with stress of less than  $5 \text{ MDyne/cm}^2$ . This is probably because the diffusion length in the as-grown web is limited by quenched-in defects or impurities. However, after heat treatment (boron diffusion), the low-stress web showed very significant improvement in the diffusion length. Diffusion lengths as high as  $116 \mu\text{m}$  were measured by the surface photovoltage technique in the low-stress web after heat treatment, while in the high-stress web there was no appreciable change in the diffusion length after heat treatment.

A web solar cell run has also been completed. Due to some processing problems, the fill factors were low and cell efficiencies were only in the range of 13-15%. More web runs are in progress.

The impurity-twin-plane interaction has been investigated by conducting DLTS measurements as a function of depth on titanium-doped web crystal. Initial results indicate that the grown-in titanium impurity tends to pile up near the twin plane. About a factor of five

increase in the Ti deep-level concentration was observed near the twin planes relative to the web surface.

Electron beam-induced current (EBIC) measurements have been performed on beveled web samples to detect any recombination activity at the twin planes within the web material. Preliminary EBIC measurements indicate that twin planes in web show higher recombination activity compared to the rest of the bulk; however, this recombination activity can vary appreciably along the length of the web crystal. Although this first set of EBIC measurements suggests that on the average the twin planes in the Ti-doped web crystal are less active, it is not clear that this observation has anything to do with Ti impurity. The variation in recombination activity along the twin planes suggests that the observed difference in the twin plane activity in the Ti-doped and baseline samples could be seen in different baseline web crystals. In addition, the DLTS measurements as a function of depth indicate an increase in the titanium deep-level concentration near the twin planes, which should, if anything, tend to increase recombination activity near the twin planes. More EBIC measurements on different web crystals are being planned to obtain a better understanding of this phenomenon.

It is important to realize that although some recombination activity has been detected at the twin planes by EBIC measurements, it is not known at this time how much impact, if any, this has on cell efficiency. In the future, an attempt will be made to correlate the two.

## 2. INTRODUCTION

The idealized efficiency<sup>(3)</sup> of a silicon solar cell is about 25%, assuming the best material and surface parameters achievable to date, although present day cells fall considerably short of this limiting value. This is largely a consequence of heavy doping effects, bandgap narrowing, and high recombination at and near the cell surfaces. The major problems of efficiency improvement fall in the above categories; however, additional design requirements are essential for efficient contacts and antireflective coating. Although these areas are well understood, they are not insignificant and must be optimized consistent with device structure.

Starting material is equally important for high-efficiency cells because device fabrication and design are academic if the starting material quality is poor or it degrades rapidly with processing. The objective of this program is to understand and improve web silicon so that high-efficiency web cells can be fabricated using advanced cell design and processing.

It is clear that high efficiency is a major attribute that will enhance the large-scale applicability of photovoltaic systems. Systems calculations indicate that for very large-scale terrestrial applications,  $\geq 15\%$  efficient photovoltaic modules will be required at a cost of  $\sim 50\text{¢/watt}$ . This implies that  $\sim 18\%$  efficient cells will be needed at low cost. Dendritic web silicon is a single-crystal silicon ribbon that has great potential for low-cost and high-efficiency solar cells. In this program we are trying to understand the loss mechanisms in dendritic web silicon by investigating the electrical activity of twin planes, the role of impurities and defects in web, impurity interaction with twin planes, starting web material quality, and the effect of heat treatment

and gettering on web quality. An improved understanding of the above effects should lead to fabrication of ~18% efficient web cells with good uniformity. This second quarterly describes progress toward the development of high-efficiency solar cells on web silicon.

### 3. TECHNICAL PROGRESS

#### 3.1 Effect of Residual Stress on Web SPV Diffusion Length

Investigations have begun regarding the relationship between residual stress and minority-carrier diffusion length in web material. Web material was acquired that has a "zero" residual stress, i.e., residual stress which has a magnitude less than 5 MDyne/cm<sup>2</sup>. In addition, the "zero" stress material also has a low (Sirtl) etch pit density, indicating a low dislocation density. The diffusion length was measured on three web crystals with different residual stress and etch pit density, both in the as-grown state and after a BBr<sub>3</sub> diffusion at 960°C. The results are summarized in Table 1. The as-grown diffusion length ranged from 9 to 40 μm. Surprisingly, the R-461 samples had the lowest diffusion length, as-grown, in spite of having the lowest etch pit density and "zero" stress. However, after the samples had gone through boron diffusion, the Z-025 material, which had the highest residual stress and etch pit density, showed no improvement, while the "zero" stress Z-028 and R-461 material improved substantially in several cases. Perhaps the most dramatic improvement was observed for sample R-461-5.13, where the diffusion length increased from 10 μm, as-grown, to 83 μm after boron diffusion.

The reproducibility of the SPV measurement is typically 10% and occasionally 20%, as determined by repeating the measurement without changing the position of the SPV probe. However, after BBr<sub>3</sub> diffusion the diffusion length was observed to vary over the surface of a web sample approximately 3 cm x 3 cm in size. For example, at four points of the Z-028-12.16 sample the measured values were 56, 110, 123, and 162 μm. This indicates that the web material quality was somewhat nonuniform in cases where the diff. ion length had reached a high

Table 1

Effect of Residual Stress and Boron Diffusion on Diffusion Length in Web Silicon (P-Type,  $4 \times 10^{14}$  ohm-cm)

Crystal	Residual Stress	Etch Pit Density	Diffusion Length As-Grown	Diffusion Length After $\text{BBr}_3$
Z-025-3.4	$14 \text{ MDyne/cm}^2$	$30,000/\text{cm}^2$	$19 \text{ } \mu\text{m}$	$16 \text{ } \mu\text{m}$
Z-025-3.10	40	30,000	16	23
Z-025-3.15	42	30,000	16	12
Z-028-12.4	< 5	2,500	25	27
Z-028-12.10	< 5	2,500	40	-
Z-028-12.16	< 5	2,500	33	116
R-461-5.3	< 5	500	17	39
R-461-5.8	< 5	500	9	-
R-461-5.13	< 5	500	10	83

NOTE:

Crystal Z-025 was grown with J435 configuration and crystals Z-028 and R-461 were grown with J460L configuration.

value. The samples listed in Table 1 are to receive a  $\text{POCl}_3$  diffusion and then be processed into finished cells. The SPV diffusion length will be measured after the  $850^\circ\text{C}$   $\text{POCl}_3$  diffusion and after the cell is completed to see if the diffusion lengths measured after  $\text{BBr}_3$  diffusion are maintained.

At this time it appears that web material, as-grown, has a diffusion length which may be much different from the diffusion length in the finished cell. Structural imperfections, as revealed by etch pits, may play a role in the way web material responds to high-temperature processing steps. The observation from the three web crystals that were examined is that the diffusion length tended to improve with the  $960^\circ\text{C}$  diffusion for web material with low residual stress, and not for material with high residual stress.

### 3.2 Dendritic Web Silicon Solar Cell Fabrication

The first web solar cell run was completed with planar geometry and oxide surface passivation. Due to some processing problems, the majority of the cells had low fill factor and cell efficiency only in the range of 13-15%. Lighted I-V data for some representative cells from this run are shown in Table 2. Cells with low fill factor generally showed high series resistance which remained even after sintering. Some more web runs have been initiated and the data from this run are being analyzed.

### 3.3 Interaction Of Twin Planes With Grown-In Impurities

#### 3.3.1 DLTS Measurements on Schottky Barrier Diodes Fabricated on Beveled Web Surface

An experiment has been designed to determine if impurities tend to be gettered by the twin planes in dendritic web silicon. Web material (p-type) has been grown with harmful impurities intentionally introduced by contaminating the silicon melt. Titanium and vanadium impurities were grown-in since the trap parameters of these impurities



Table 2. Dendritic Web Silicon Solar Cells

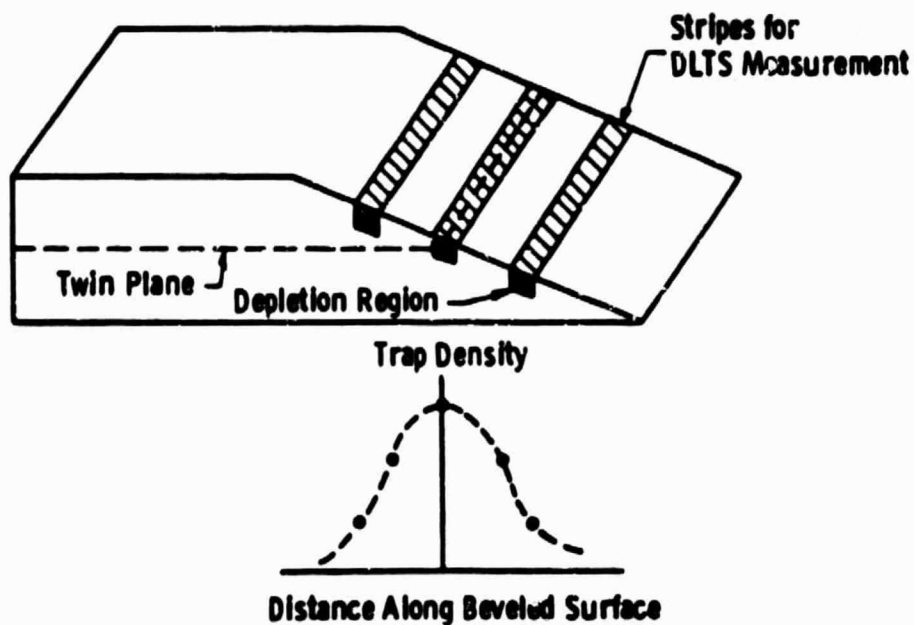
Cell ID	$J_{sc}$ mA/cm <sup>2</sup>	$V_{oc}$ mV	FF	$\eta$ %
32-1	31.70	.584	.785	14.60
32-2	31.70	.581	.792	14.70
2-2	30.00	.590	.800	14.20
2-3	30.00	.590	.799	14.10
2-5	29.60	.582	.756	13.10
76-2	35.30	.543	.744	14.30
28-2	36.00	.550	.762	15.20
A-1	30.78	.548	.689	11.63
*FZ-cell	35.00	.609	.801	17.10

\*FZ cells were fabricated with the web run.

are well known. These impurities will act as internal tracers in the study of twin plane-assisted internal gettering when the web material is subjected to various heat treatments.

Schottky diodes, in the form of stripes, were fabricated by depositing Ti/Au on a beveled web surface as shown in Figure 1. DLTS measurements, performed on the stripe covering the twin plane and on adjacent stripes, provides a profile of the trap concentration. If impurities do pile up at the twin plane and remain electrically active, a profile as shown in Figure 1 will be observed.

Dwg. 9357A97



- Use a Grown-In Impurity (Ti, V) as an Internal Tracer
- Observe Trap Density as a Function of Distance from Twin Plane, Both As-Grown and After Processing (Including Gettering)
- Compare Web Having High Diffusion Length with Web Having Low Diffusion Length (As Determined by SPV) Using this Technique

Figure 1. DLTS detection and identification of impurities piled up at the twin plane.

To date, approximately ten 2 x 5 mm pieces have been cut from the Ti-doped web crystal. These pieces have been beveled at an angle of  $2^{\circ} 52'$  and polished to remove surface damage. Part of the beveled surface was then etched to reveal the location at which the twin planes emerged from the beveled surface. A photograph of one such sample is shown in Figure 2.

A mask was designed and fabricated for this purpose. The width of the stripes is 125  $\mu\text{m}$  and the spacing is 25  $\mu\text{m}$ , giving a depth resolution of 7.5  $\mu\text{m}$  from stripe to stripe. There are 30 stripes in a set, and the mask has stripe lengths of 1.0 mm, 1.5 mm, and 2.0 mm to accommodate samples of different size. The mask layout is shown in Figure 3. In addition to the stripes, larger rectangles are included in the mask to aid in proper alignment of the stripes with the twin plane.

In addition to the Ti-doped web samples, standard silicon web samples were also cut and beveled for comparison. After deposition of the DLTS stripes, the samples were mounted in a TO-5 header for the DLTS measurements.

On the as-grown titanium-doped web material (J167-1.1), the diffusion length was measured by the surface photovoltage technique to be 22  $\mu\text{m}$ , compared to the diffusion length in standard as-grown web material, which falls in the range of 8 to 74  $\mu\text{m}$ . Thus, the diffusion length is low for titanium-doped web but not extraordinarily low, suggesting that the concentration of titanium in the web was not extremely large. In order to measure this concentration, a conventional DLTS measurement was made using a 30-mil diameter Schottky diode as the test device. This dot, consisting of titanium and gold, was evaporated directly on the as-grown silicon surface. The results are shown in Figure 4, where two DLTS peaks are evident. Several scans were made in order to calculate the energy level associated with each peak, although only one scan is shown in Figure 4. The position in temperature and the energy level associated with peak 2 agree with those previously obtained for titanium in silicon. The concentration of titanium is  $1.7 \times 10^{12} \text{ cm}^{-3}$ ,

ORIGINAL PAGE IS  
OF POOR QUALITY

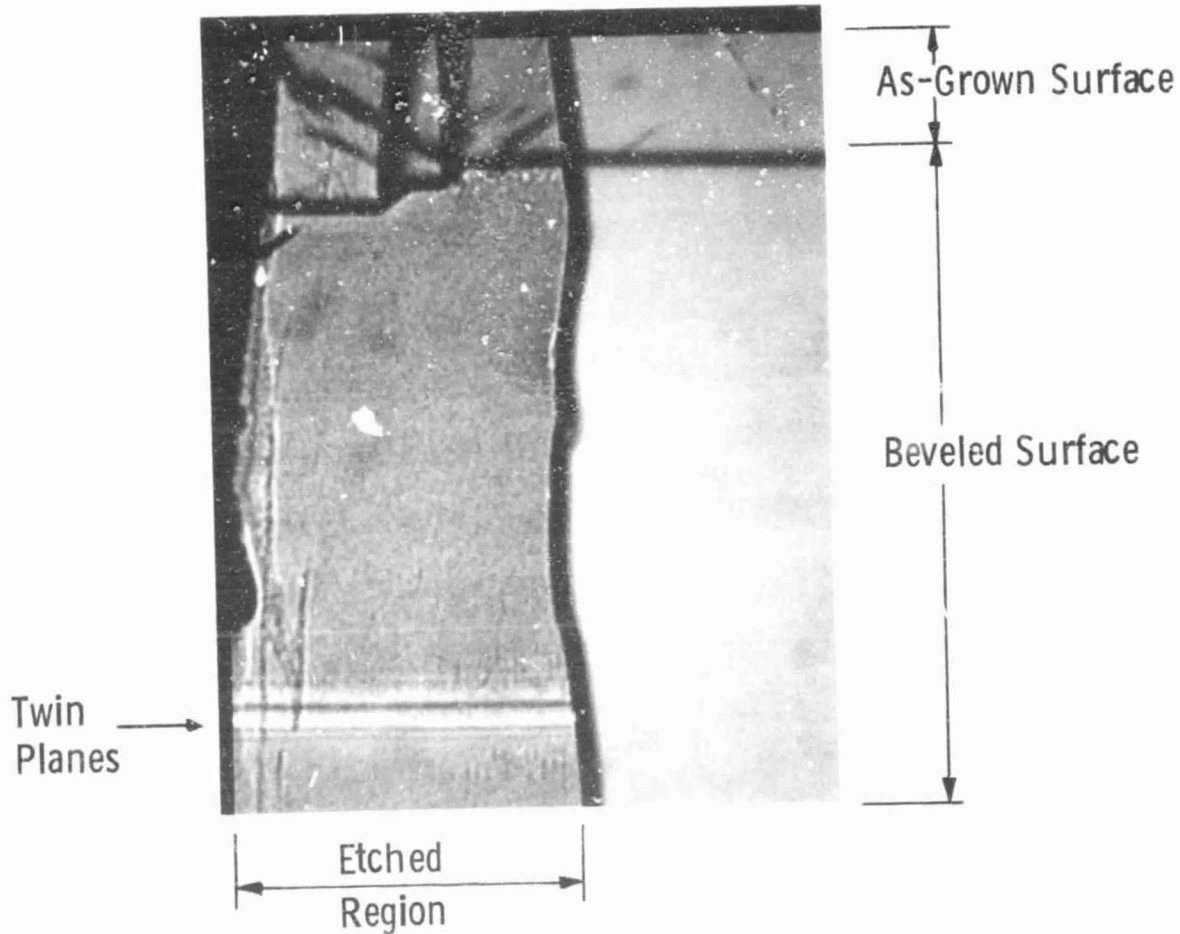


Figure 2. Optical photograph (50X) of beveled sample for Ti-doped web crystal J167-1.1 (run TP-3, sample T-1).

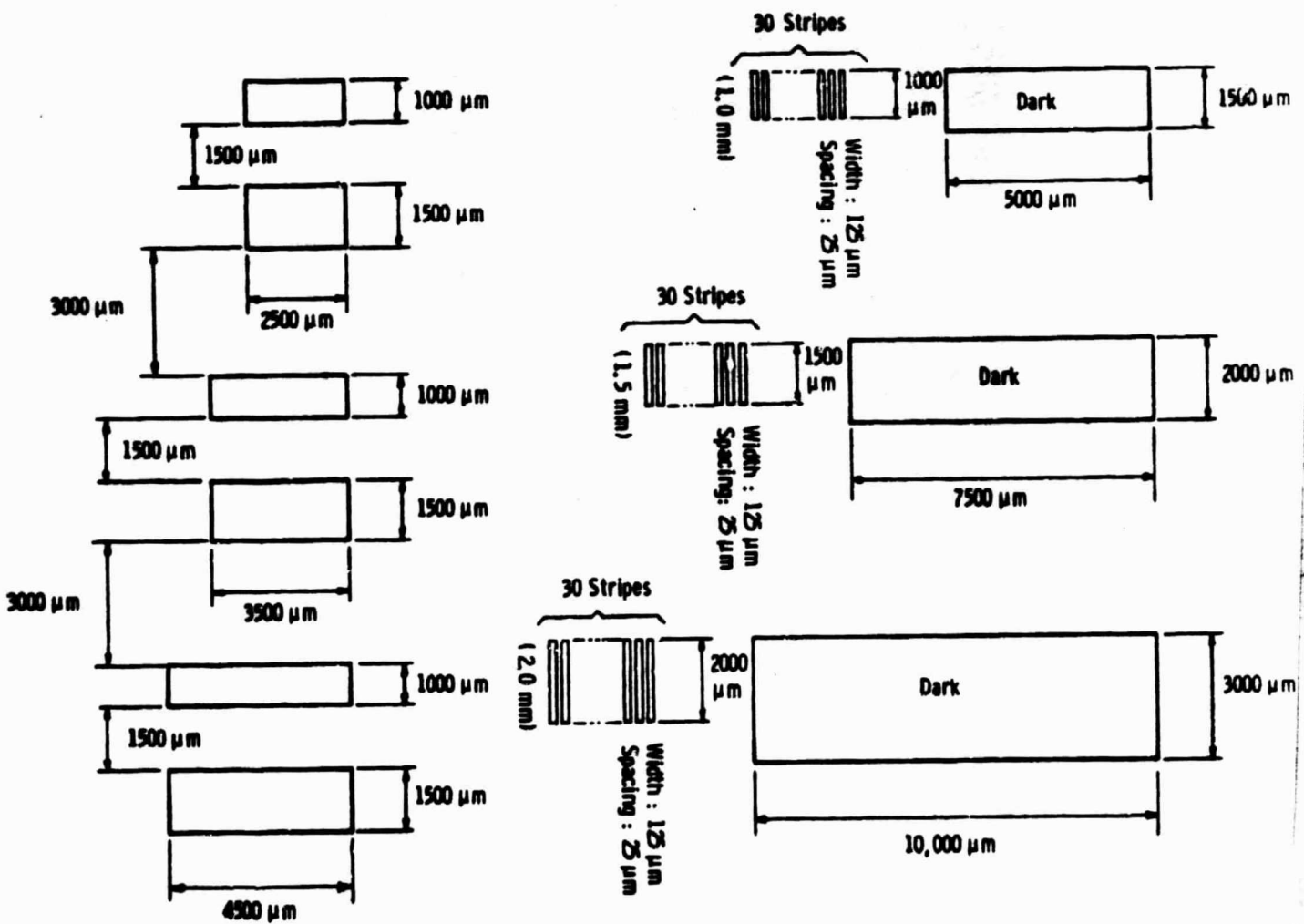


Figure 3. Mask for twin plane activity.

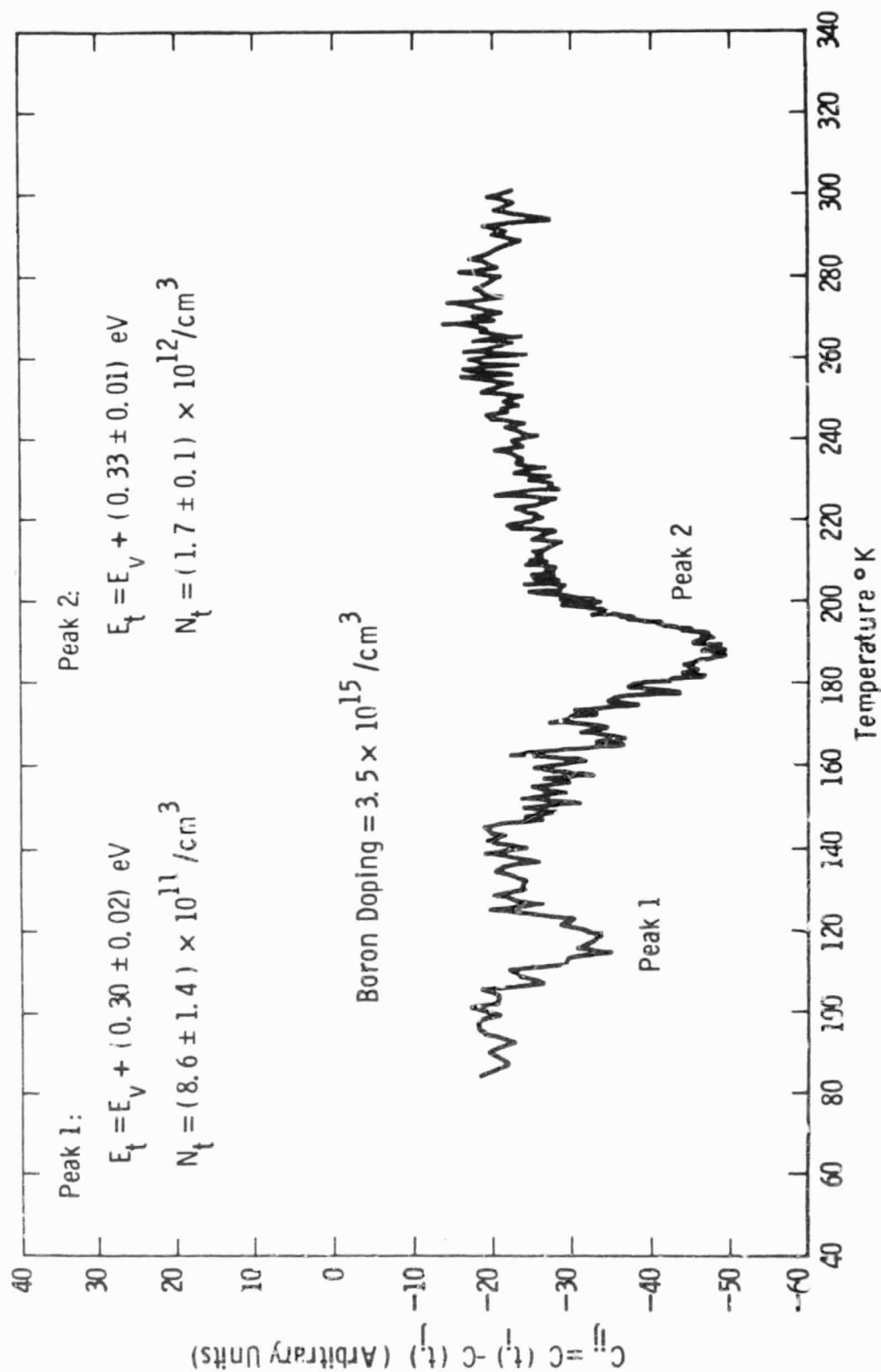


Figure 4. DLTS scan for Ti-doped web crystal J167-1.1, as grown. Test device is a 30-mil Schottky dot.

which is only a factor of five above the detection limit of  $3.5 \times 10^{11}/\text{cm}^3$  for 5 ohm-cm material. The source of peak 1 in Figure 4 at this time is not known.

DLTS measurements were then made on a beveled sample with titanium doping. In this case the Schottky diode was in the shape of a stripe  $125 \times 1000 \mu\text{m}$  in size. The stripes were defined by photolithography and were placed on the beveled surface as well as on the unbeveled, as-grown surface. One stripe was located directly over the line at which the twin planes emerged from the beveled surface. Attempts were made to make DLTS measurements at three stripes (Figure 1): one over the twin planes, another near the top of the beveled surface, and a third on the unbeveled surface. In all three cases, the DLTS peak for titanium was not detected. There are two possible reasons for this. The area of the stripes is  $200 \text{ mil}^2$  compared to the area of the standard DLTS dot, which is  $706 \text{ mil}^2$ . Thus, a factor of three in sensitivity is lost when the stripes are used for greater spatial resolution. The second reason is that the leakage current for the striped Schottky diodes was large, with  $500 \mu\text{A}$  of current flowing at a reverse bias of 4 volts. This leakage current supplies a continuous flow of majority carriers past the traps in the depletion region. These majority carrier traps then tend to be filled by the leakage current rather than by the DLTS bias pulse, and this further degrades the sensitivity of the measurement. When the beveled samples were mounted on a TO-5 header and wire bonds were made from the stripes to the pins on the TO-5 package, the leakage currents were quite good, with a typical value of  $20 \mu\text{A}$  at a reversed bias of 6 volts. The reason for the striped Schottky diodes degrading in leakage current is not known at this time. It is anticipated that leakage current will be limited to acceptable values for future Schottky striped diodes so that the titanium impurity will be more easily detected.

### 3.3.2 DLTS Measurements on Schottky Barrier Diodes Formed After Step Etching the Ti-Doped Web Crystal

In order to investigate the twin-plane-impurity interaction and because of some difficulty in the above experiment, an alternate approach was used in which titanium-doped web crystal was etched to various depths (0, 0.4, 1, 2, and 3 mils) to obtain a depth profile of Ti concentration. In this experiment conventional Ti-Au Schottky dots (30-mil diameter) were used as DLTS test devices and, because of the large area and low leakage current, there was more success in detecting Ti as a function of depth. It should be recognized that the DLTS concentration of Ti in a CZ-type material is only about 40% of the total grown-in Ti concentration in the bulk.<sup>(1)</sup>

Figure 5 shows the depth profile of the electrically active Ti concentration. The data show a monotonic rise in the titanium deep-level concentration approaching the twin planes from the web surface. The twin planes are about 3 mils below the surface, suggesting that the grown-in impurities tend to pile up near the twin planes. In the case of Ti impurities, there is a difference of about a factor of five between the concentration near the twin planes and at the surface.

### 3.4 Electron-Beam-Induced Current (EBIC) Measurements to Investigate the Recombination Activity at the Twin Planes in Web Silicon

The first quarterly report<sup>(1)</sup> showed laser-beam-induced current (LBIC) measurements on a couple of web crystals. LBIC measurements on those web crystals did not reveal any excess recombination activity at the twin planes, but one side of the twin plane showed more recombination than the other half. More LBIC measurements are being performed on baseline and Ti-contaminated web crystals to obtain further information about any twin plane recombination activity.

In this section is shown a first attempt to look at the twin plane activity by electron-beam-induced current (EBIC) measurements. These measurements were performed at SERI on beveled web surface<sup>(2)</sup> by fabricating 500 Å Al Schottky barriers on the beveled surface and 1000 Å Au ohmic contact on the back surface.



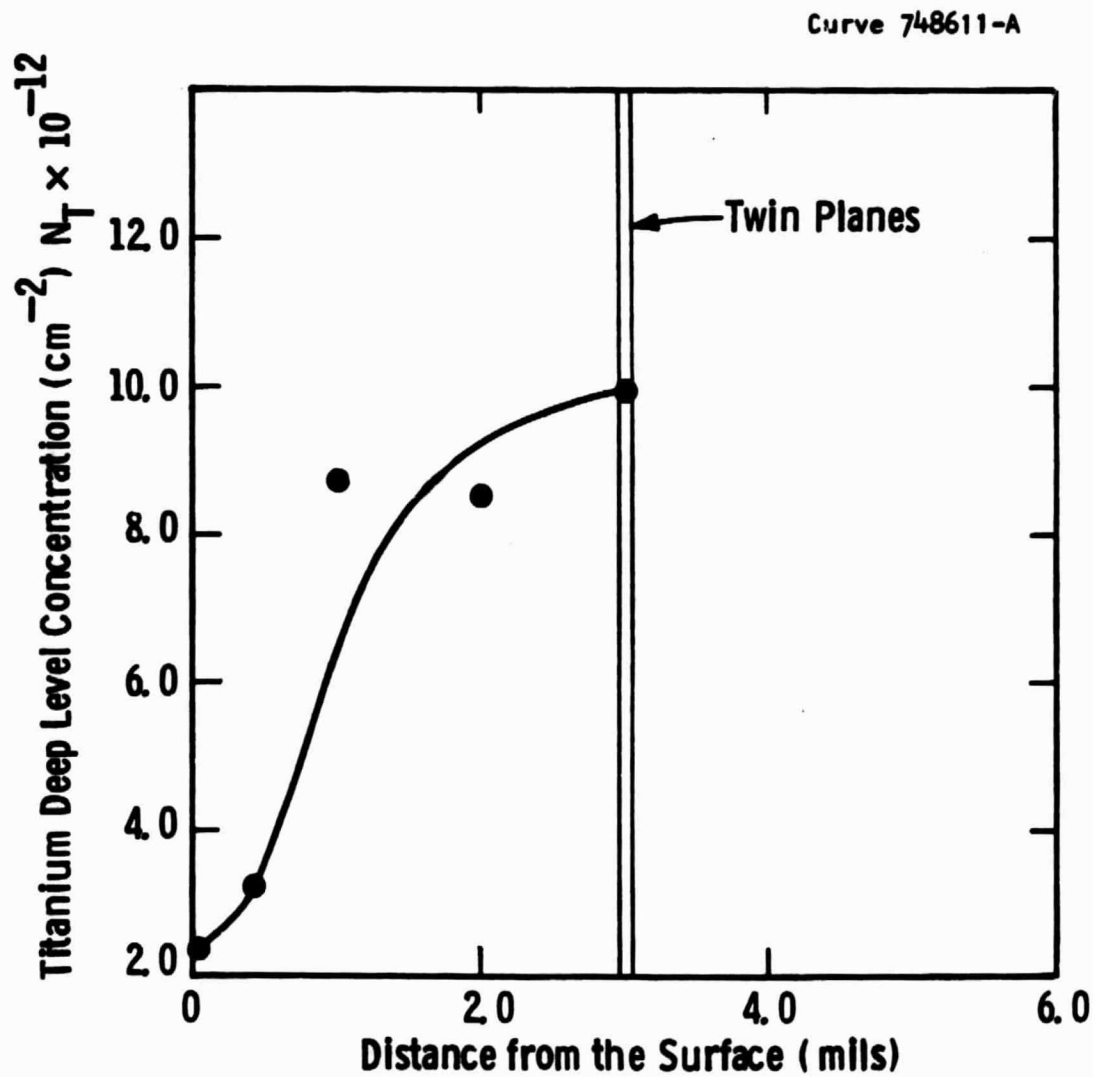


Figure 5. DLTS study of the interaction between grown-in titanium impurity and the twin planes in dendritic web silicon.

As shown in the optical photograph of Figure 2, part of the mechanically polished beveled surface was protected, while the other part was chemically etched to reveal the twin planes. EBIC scans were performed on both chemically etched and mechanically polished regions of a baseline web crystal, R461-4, and a Ti-contaminated web crystal, J167-1.3-TP3#8.

#### 3.4.1 EBIC Measurements on Baseline Web Crystals

Figure 6 shows an EBIC picture of the baseline R461-4 web, where the chemically etched portion is in the dark area but the mechanically polished region can be seen clearly with the active twin planes. This EBIC picture also shows that a section of the twin plane is not as dark or electrically active as the rest of it. Also apparent is contrast due to some sort of a film and scratch-like marks on this sample. EBIC scans have been attempted through the section of the twin planes in the a) chemically etched region, b) mechanically polished region where the twin planes look dark, and c) mechanically polished region where the twin planes look relatively lighter.

Figure 7 shows the EBIC scan through the twin planes in the chemically etched region. A drop in the electron-beam-induced current is seen clearly at the two twin planes within this web crystal, indicating excess recombination at the twin planes compared to the rest of the bulk. The hysteresis in the current scan has something to do with the instrumentation since this is observed in all cases.

Figure 8 shows the EBIC on scan sample R461-4 through the section of polished region which is located ~ 400  $\mu\text{m}$  away from the boundary of the etched and polished region. It is clear that the two twin planes look dark and show about 40% reduction in current, indicating considerable recombination at the twin planes. Recombination at the twin planes in this region is about a factor of three greater than the twin planes in the etched region (Figure 7).

ORIGINAL PAGE IS  
OF POOR QUALITY

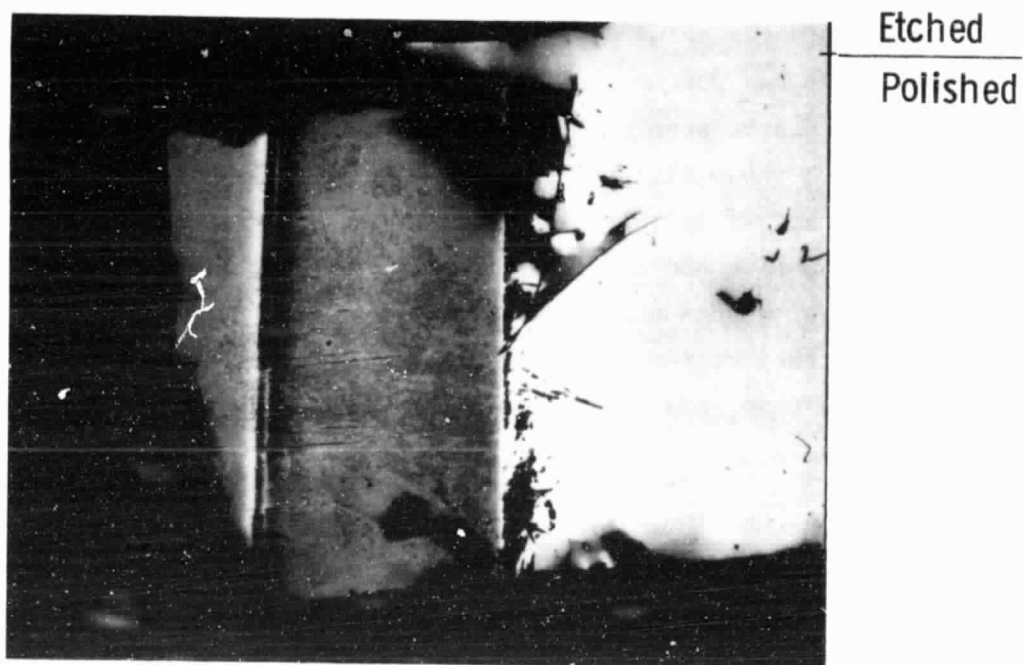


Figure 6. Electron-beam-induced current (EBIC) picture of the beveled baseline web crystal R461-4. Twin planes can be seen on the polished beveled surface.

ORIGINAL PAGE IS  
OF POOR QUALITY

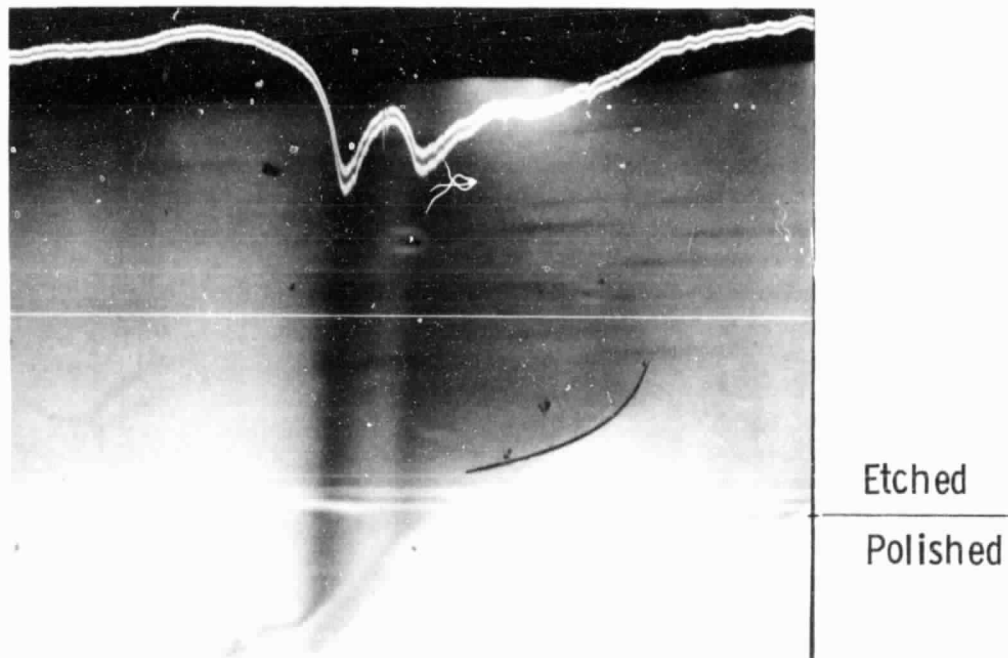


Figure 7. EBIC scan through the twin planes on the chemically etched region of the beveled web surface of baseline crystal R461-4 ( $I_D \sim 270$  pA).

ORIGINAL PAGE IS  
OF POOR QUALITY

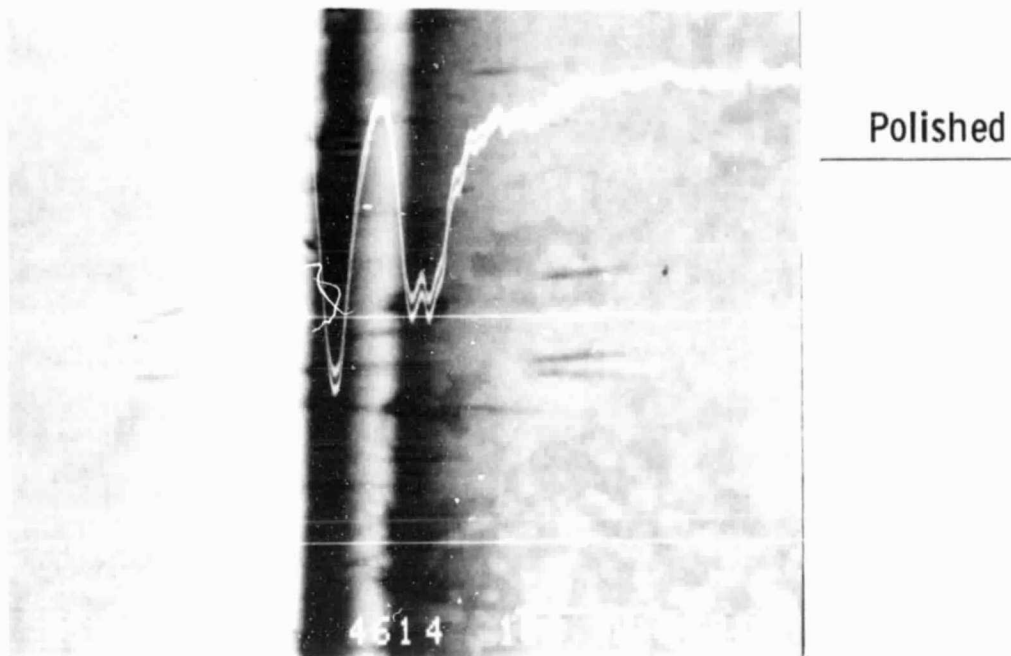


Figure 8. EBIC scan through the twin planes located on the polished beveled web surface of crystal R461-4. Scan is taken 400  $\mu\text{m}$  away from the etched region ( $I_b = 270 \text{ pA}$ ).

Figure 9 shows the EBIC scan on sample R461-4 through the section of the polished region which is 700  $\mu\text{m}$  from the bottom edge (Figure 6) and where the twin planes look somewhat lighter in contrast. Figure 9 shows that in this region one of two twin planes is not very electrically active, while the other twin plane shows the same amount of recombination as in Figure 8.

Thus it appears that although the twin planes are active, the recombination activity at the twin planes can vary considerably along the length of a web crystal.

#### 3.4.2 EBIC Measurements on Titanium-Doped Web Crystal

Figure 10 shows an EBIC scan of the Ti-doped web crystal J167-1.3-TPE3#8, which was taken in the chemically etched region. The current scale magnification was the same as in the baseline crystal. In this region of the crystal some recombination activity is seen at the twin plane, but this activity is smaller than what was seen in the etched region of the baseline crystal (Figure 7).

Figure 11 shows an EBIC scan in the polished region of the Ti-doped crystal where somewhat more recombination at the twin planes is observed compared to what was seen in the etched region (Figure 10). The recombination activity in this figure also looks somewhat less than in the baseline samples of Figures 8 and 9.

ORIGINAL PAGE IS  
OF POOR QUALITY

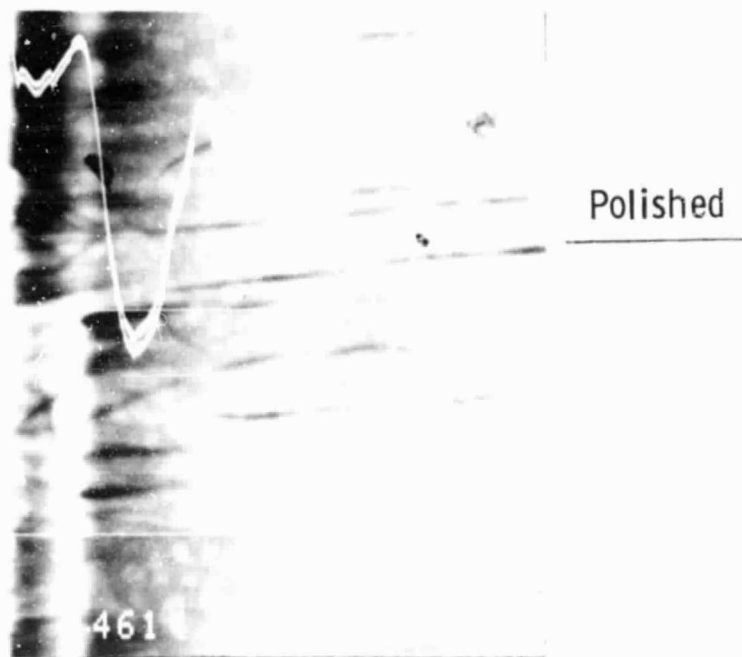


Figure 9. EBIC scan through the twin planes located on the polished web surface of crystal R461-4. This scan was taken 700  $\mu\text{m}$  away from the bottom edge ( $I_b = 270 \text{ pA}$ ).

ORIGINAL PAGE IS  
OF POOR QUALITY

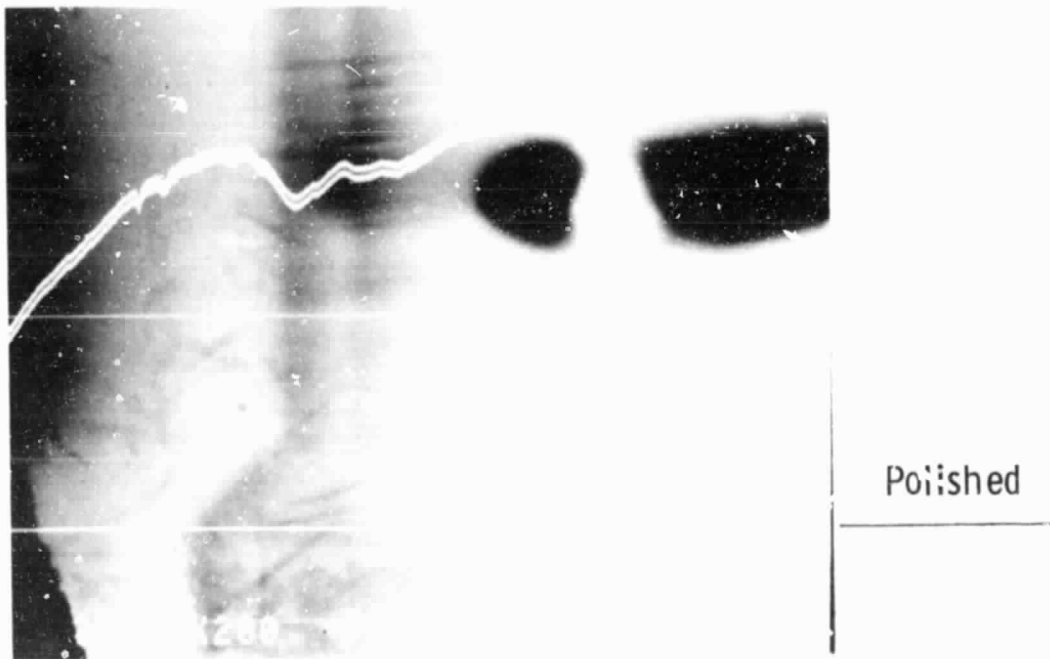


Figure 10. EBIC scan through the twin planes located on the chemically etched region of the beveled web surface of Ti-doped web crystal J167-1.3-TP3#8.



ORIGINAL PAGE IS  
OF POOR QUALITY

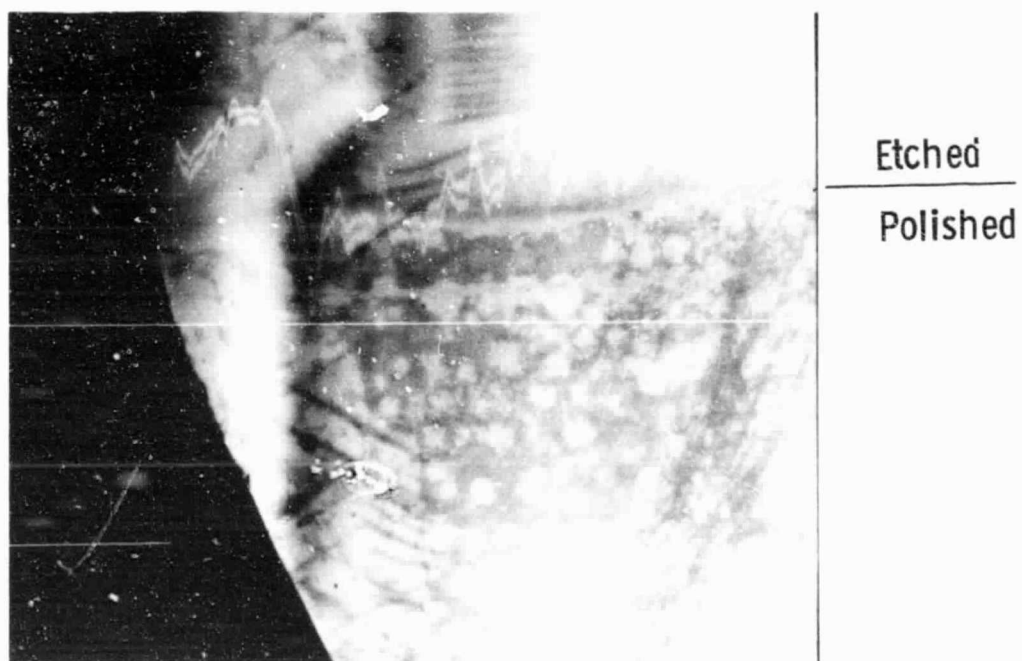


Figure 11. EBIC scan through the twin planes located on the polished region of the beveled web surface of Ti-doped web crystal J167-1.3-TP3#8.

#### 4. PROGRAM STATUS

##### 4.1 Present Status

The current milestone chart for this program is shown as Table

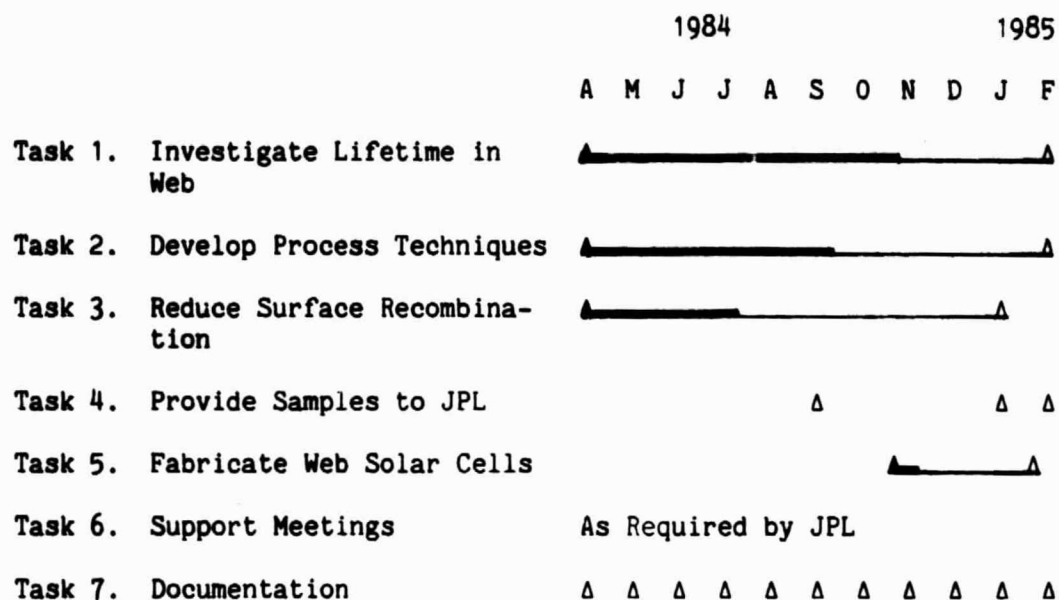
3. During this period we have:

- Studied the effect of stress on diffusion length in web crystals.
- Studied the twin-plane-impurity interaction by DLTS measurements on Ti-doped doped web crystal.
- Investigated the recombination activity at the twin planes by EBIC measurements.
- Fabricated some web solar cells.

##### 4.2 Future Activity

Plans are to conduct more LBIC and EBIC measurements to understand the recombination activity of the twin planes and its impact on web cell performance. Heat treatment studies on web will continue with more emphasis on high-efficiency web cell fabrication.

Table 3  
MILESTONE CHART



## 5. REFERENCES

1. A. Rohatgi et al., "A Study of Grown-In Impurities in Silicon," J. Solid State Electronics, Vol. 26, No. 11, p. 1039 (1982).
2. A. Rohatgi, D. L. Meier, R. B. Campbell and P. Rai-Choudhury, First Quarterly Report on "Development of High-Efficiency Solar Cells on Silicon Web," JPL Contract No. 956786.
3. A. Rohatgi and P. Rai-Choudhury, IEEE Trans. on Electron Devices, ED-31, No. 5, p. 569 (1980).

## 6. ACKNOWLEDGMENTS

The authors would like to thank T. F. Ciszek, Rik Matson, and Terry Schnyder of SERI for their excellent job on EBIC measurements. They would like to thank J. B. McNally, F. S. Youngk, and G. J. Machiko for cell fabrication; W. Cifone for the preparation of beveled web pieces of LBIC measurements; T. W. O'Keeffe for assistance with the LBIC measurements; S. Karako for surface photovoltage measurements and assisting with the model calculations; and G. S. Law for reading and preparing the manuscript.